Horizons of modern molecular dynamics simulation in digitalised solid freeform fabrication with advanced materials

Saurav Goel[1,2,3,4*], Michael Knaggs[2], Gaurav Goel[1,2], Xiaowang W. Zhou[5], Hari M Upadhyaya[1], Vijay Kumar Thakur[4,6], Vinod Kumar[2], Gregory Bizarri[2], Ashutosh Tiwari[7], Adrian Murphy[8], Alexander Stukowski[9] and Allan Matthews[10]

[1] *London South Bank University, London, SE10AA, UK*
[2] *Cranfield University, Cranfield, MK43 0AL, UK*
[3] *EPSRC Centre for Doctoral Training in Ultra-Precision Engineering, University of Cambridge and Cranfield University, UK*
[4] *Shiv Nadar University, Gautam Budh Nagar, 201314, India*
[5] *Sandia National Laboratories, Livermore, CA 94550, USA*
[6] *Biorefining and Advanced Materials Research Center, Scotland's Rural College (SRUC), Kings Buildings, Edinburgh, EH9 3JG, UK*
[7] *The University of Sheffield, S1 3JD, UK*
[8] *Queen's University Belfast, BT95AH, UK*
[9] *Darmstadt University of Technology, Darmstadt, D-64287, Germany*
[10] *The University of Manchester, Manchester, M13 9PL, UK*

*Corresponding author Tel.: +44 020 7815 7581, Email address: GOELS@LSBU.AC.UK

Abstract:

Our ability to shape and finish a component by combined methods of fabrication including (but not limited to) subtractive, additive and/or no theoretical mass-loss/addition during the fabrication is now popularly known as solid freeform fabrication. Fabrication of a telescope mirror is a typical example where grinding and polishing processes are first applied to shape the mirror and thereafter an optical coating is usually applied to enhance its optical performance. The area of nanomanufacturing cannot grow without a deep knowledge of the fundamentals of materials and consequently, the use of computer simulations is becoming ubiquitous. This article is intended to introduce the most recent advances in the computation benefit specific to the area of solid freeform fabrication as these systems are traversing through the journey of digitalisation and Industry-4.0. Specifically, this article demonstrates that the application of the latest materials modelling approaches, based on techniques such as molecular

1

dynamics, are enabling breakthroughs in applied precision manufacturing techniques.

Keywords: MD simulation; Solid freeform fabrication; additive manufacturing; digital manufacturing

Acronyms:

3DAP	3D atom probe
AMBER	Assisted Model Building with Energy Refinement
ASIC	Application Specific Integrated Circuits
BOP	Bond order potential
CAT	Crystal Analysis tool
CHARMM	Chemistry at HARvard Macromolecular Mechanics
CFD	Computation fluid dynamics
CPU	Central processing unit
DXA	Dislocation extraction algorithm
FEA	Finite element analysis
FPGA	Field Programmable Gate Arrays
GMR	Giant magneto-resistive
GPU	Graphics processing unit
HPC	High-performance computing
LAMMPS	Large scale atomic massively parallel simulation
LJ	Lennard Jones
MEB	Molecular beam epitaxy
MD	Molecular dynamics simulation
NAMD	Nanoscale molecular dynamics
NEMD	Non-equilibrium molecular dynamics
PME	Particle mesh Ewald

PoP	Package-on-package
PPPM	Particle-Particle Particle-Mesh
R2R	Roll to Roll fabrication
SFF	Solid freeform fabrication
SiP	System-in-package
SoC	System on chip
SIMD	Single instruction multiple data model
vdW	van der Waals Forces

1.0. The emergence of digitalisation in micro-manufacturing

In-situ monitoring of microfabrication technologies has become crucial in the age of nanoscale digital manufacturing. While experimental efforts are still underway [1], the emergence of newer kinds of materials (auxetic materials, metamaterials, 2D materials, scintillating and doped materials in heterogenous ratios) that can predictably be modelled with the known physics of *ab-initio* methods, it is now a practice to simulate new material ahead of experimental synthesis to identify the incentives associated with scalable developments in the manufacturing of such materials. In this spirit, various simulation tools have emerged over the past decades, including advances in macroscopic combinatorial coupling schemes such as FEA and CFD [2] as well as methods like homogenisation in time [3, 4], Model reduction techniques [5], Movable cellular automaton [6], the Discrete element method [7] and coupling of FEM with MD simulation [8]. However, while these methods have solved the problem of the size scale, they have not succeeded in mitigating the problem of the time scale. For these reasons, molecular dynamics (MD) has continued to be the preferable tool over the last decade for the research community investigating nanoscale manufacturing.

This main simulation tools used in the past to study various tribological problems including

micromanufacturing processes was benchmarked recently in a review article and shown in Figure 1 [9]. The bottom part of the graph takes us close to the fundamental physics domain while the upper part of figure 1 takes us closer to the macroscopic engineering world. An intermittent place is occupied here by the MD that leverages quantum mechanical calculations to model atomic interactions in the material.
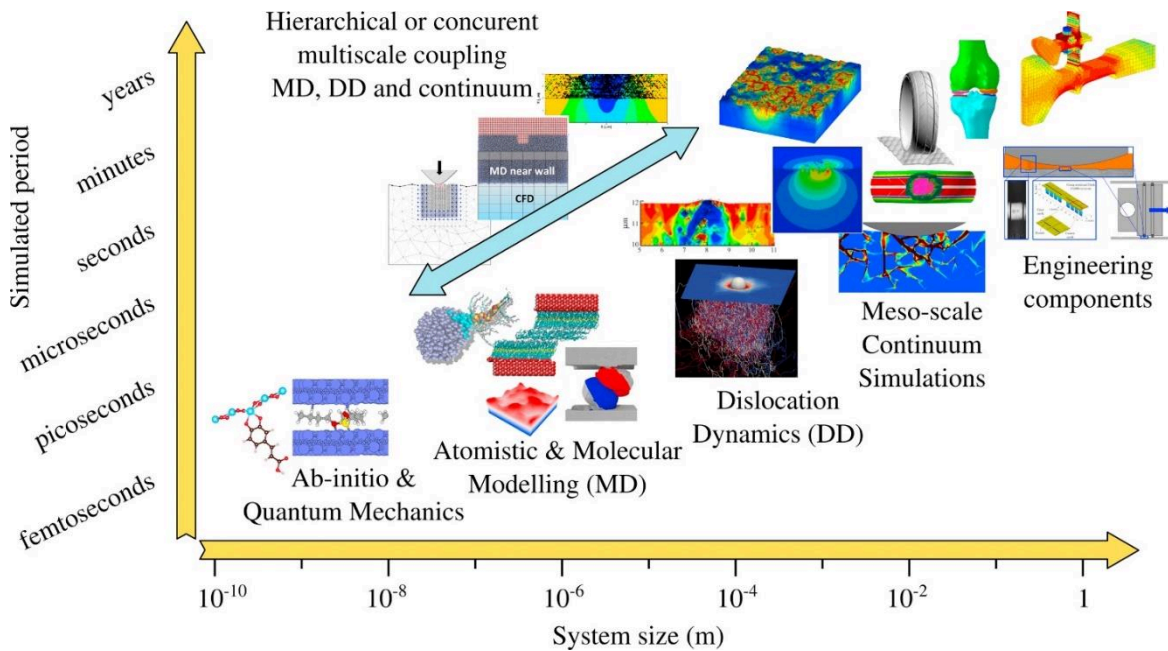

Figure 1: Time scale vs Length scale representation of various simulation methods applied to study a wide range of micromanufacturing and tribology problems, Reprinted with permission [9]

In the past, it has been alluded to that MD intermittently permits direct observation of events occurring at the atomic level, especially at short timescales of a few femtoseconds that cannot be studied using traditional engineering simulation methods like FEA. Furthermore, one principal difference between FEA and MD is that the nodes and the distances between the nodes in MDS are not selected on an arbitrary basis but based on more fundamental units of the material, namely, the position of atoms as the nodes and inter-atomic distances as the distance between the nodes. Also, the shape and size of the crystal in MDS is dictated by the

crystallographic structure of the material and not arbitrarily, such as triangular or rectangular shapes as in FEA and therefore one expects MD to provide a bottom-up understanding of the process as opposed to the top-down understanding. With new developments described in this paper, it is possible to accurately model and simulate with MD to gain a solid understanding of discrete processes such as dislocation mediated plasticity and Burgers Vectors responsible for slip on a particular crystal plane [10] and/or tribochemistry involved during the process.

MD is an iterative application of Newtonian mechanics to an ensemble of atoms and molecules. Each iteration consists of two phases, force computation and motion integration. The forces may include non-bonded (e.g., Lennard-Jones or Coulomb) and bonded terms, and are related to motion through:

$$F_{ix} = -\frac{dV}{dx_i} = m_i \cdot a_{ix} = m_i \cdot \frac{d^2 x_i}{dt^2} \tag{1}$$

where x_i and a_{ix} are the x- component of coordinate and acceleration of atom i, F_{ix} is the x-component of the interaction force on i, m_i is i's mass of the ith atom, and V is the potential energy function. In MDS, these equations are integrated by numerical techniques for extremely short time periods (~100 nanoseconds); and equilibrium statistical averages are computed as temporal averages over the observation time. To render atomistic simulation studies practical, an interatomic potential function is necessary. During MDS, the interatomic bonding forces (both attractive and repulsive) are defined by an appropriate empirical potential-energy function such that:

$$F_{total} = F_{bond} + F_{angle} + F_{torsion} + F_{non-bonded} \tag{2}$$

The bonded terms in the above equation affect only the neighbouring atoms, and their computational effort scales with the number of particles N being simulated, i.e., $\sim O(N)$.

On the other hand, the amount of computational effort needed to calculate non-bonded interactions scales as $O(N^2)$, which represents a significant computational cost. When parallelised, the long-range force can dominate further, especially for large computer systems

operating on small to medium-sized problems [11]. To reduce the computational costs associated with the calculation of non-bonded interactions, several schemes have been adopted, such as the introduction of cut-offs, where the non-bonded interactions are not calculated when the distance between two atoms exceeds the cut-off distance [12]. Van der Waals (vdW) or Lenard-Jones (LJ) non-bonded interactions are short-range in nature (for LJ these typically contain an r^{-6} term) and therefore can be approximated accurately using a distance cut-off to reduce the computational effort required from the full $O(N^2)$ computational complexity. Whereas coulombic interactions are long-range in nature (these contain an r^{-1} term) and cannot be accurately approximated using a distance cut-off scheme without corrections. Schemes for calculating coulombic interactions having lower computational complexity than $O(N^2)$ have been developed, such as Particle Mesh Ewald (PME) (N log(N)) [13] and Particle-Particle Particle-Mesh (PPPM) [14] (N log (N)$^{0.5}$). The most widely used method for calculating fast electrostatic interactions is the Ewald method, which divides the electrostatic interactions into two parts. The first decays rapidly with distance to a specified cut-off and is a direct space sum, the second decays slowly but can be expressed efficiently by taking the fast Fourier transform of the charge distribution on a regular mesh. A detailed comparison of the Ewald and PPPM methods indicates that PPPM is both easier to implement and faster than the other methods [15].

2. Latest advances in accelerated molecular dynamics

Numerous approaches have been used to accelerate classical MD simulations with different hardware technologies as described below:

2.1. Parallel computing

Parallel MD algorithms typically partition the simulation domain using spatial decomposition techniques (Figure 2). Each subdomain is assigned to a different processor with each processor sharing and storing information about "ghost" atoms in neighbouring domains which are within

the non-bonded cut-off of that processor's subdomain. Thus, the computation on each processor is performed mainly on data within the assigned subdomain and therefore local memory, minimizing the performance overhead associated with communicating information about the "ghost" atoms from neighbouring domains.
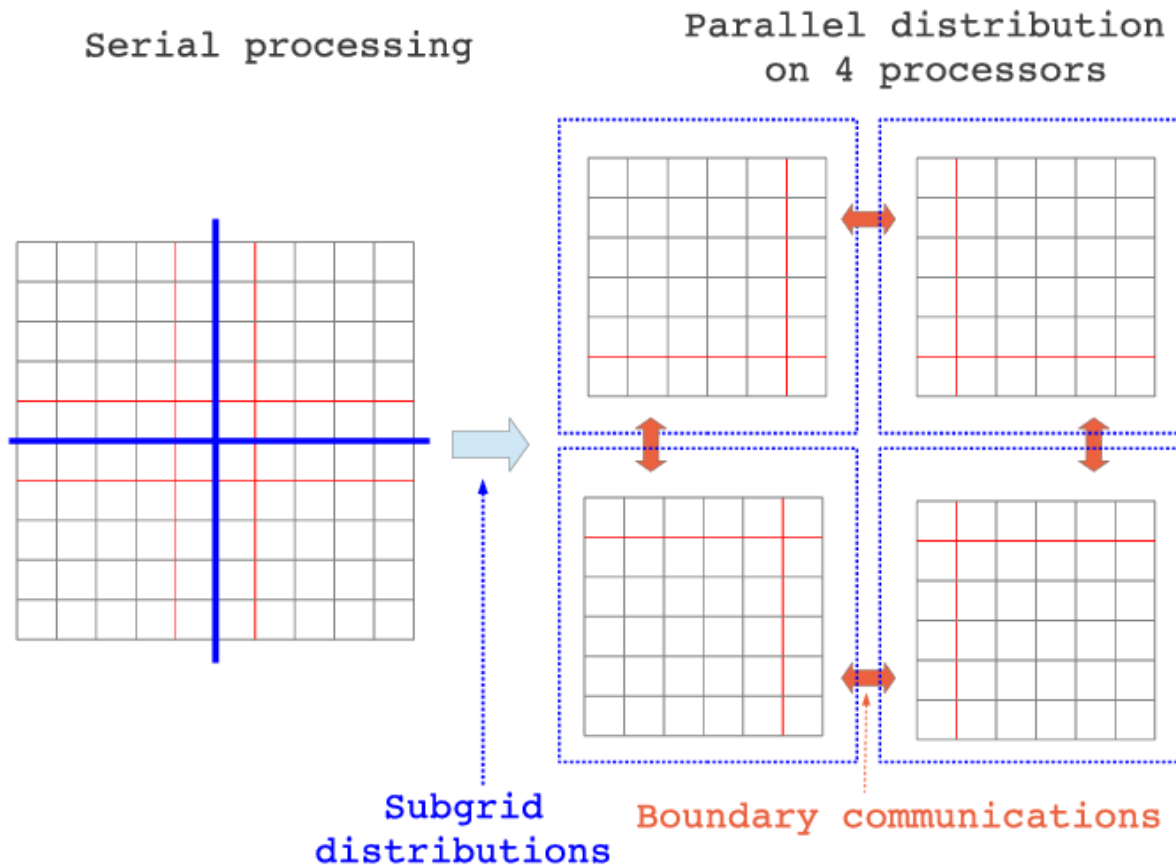

Figure 2: Diagram depicting the spatial decomposition of a 2D domain across 4 processors that can be run in parallel. Note the "ghost" regions that are duplicated between each of the 4 processors (red lines) where changes are updated between processors during the calculations using boundary communications.

2.2. Graphics Processing Units (GPUs)

As opposed to a traditional central processing unit (CPU), graphics processing unit (GPU) is an example of a massively parallel stream processing architecture which uses the single instruction multiple data model (SIMD) (Figure 3).
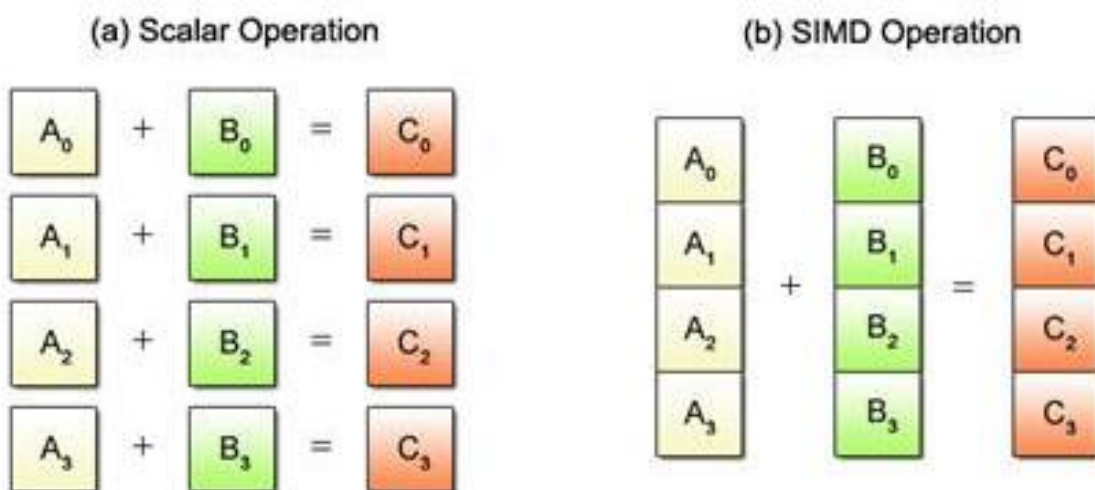
Figure 3: Diagram depicting the addition of two vectors A and B on (a) a scalar architecture (non-vector pipelined) CPU architecture (b) a single instruction multiple data (SIMD) architecture (such as a GPU). Note that the operations on a SIMD architecture are performed in parallel as a single operation running on multiple CPUs whereas on the scalar architecture each or the operations are performed in sequence.

A typical GPU contains thousands of very simple processing units. However, unlike CPUs, these are optimized for streaming numerical operations in "lock-step" and there is usually a large performance penalty for any conditional branching operation (such as an if, case or while statement). For efficient use of the GPU hardware, algorithms must be written to make the most of the inherent vectorization in the hardware. GPU cores typically have access to a small amount of cache memory and a global device memory which can be accessed by all GPU cores. As with CPUs accessing the cache memory lower latency is involved than when accessing the global device memory. When these factors are considered it is apparent that an in-depth understanding of the architecture of the GPU hardware is required to take advantage of the raw computation performance the hardware offers. The fine-grained parallelism of MD algorithms makes them an ideal candidate for implementation on GPUs. GPUs offer significant computational performance at the cost of increased programming complexity compared with CPUs. Presently, a variety of MD codes takes advantage of GPU acceleration, for example, NAMD [16], LAMMPS [17], AMBER [18] and CHARMM [19].

2.3. Field Programmable Gate Arrays (FPGA)

A Field Programmable Gate Arrays (FPGA) is an integrated circuit designed to be configured by a customer or a designer for customised manufacturing. As such, they allow the hardware to be reconfigured to meet user requirements. Most FPGA based approaches to accelerating molecular dynamics codes use multiple custom pipelines per CPU core to accelerate the calculation of the non-bonded interaction components of the force field. For example, one such design used 4 non-bonded interaction pipelines per CPU to accelerate a version of LAMMPS. Speedups of up to 15x have been achieved with respect to CPU based calculations. Unfortunately, a specialised skill base is required to achieve these levels of performance when using FPGAs relative to approaches that use CPU's and/or GPUs for accelerating molecular dynamics simulations. Typically, approaches that use OpenGL and the FPGA vendors' tool chain to automatically design hardware within the FPGA do not result in high efficiency. A hardware design element is usually required.

2.4. Application Specific Integrated Circuits (ASIC)

An Application Specific Integrated Circuit (ASIC) is a circuit designed to perform a specific set of functions, which typically cannot be altered once the design is finalised. There is a long history of experimenting with ASICs as a means for accelerating molecular dynamics simulations [20, 21]. Very high levels of performance are possible using this approach. However, the development of such ASICs can be very protracted, expensive and is a very specialised pursuit. The more recent attempts that have taken this approach are in High performance supercomputers (HPC's) such as MD-GRAPE4 [22] and Anton[*]. It is interesting to note that in both HPC's, a system on chip (SoC) approach was taken, where accelerator(s), memory, general-purpose CPU and 6-way network were integrated onto a chip to reduce latency. For example, MD-GRAPE4 can calculate 51.2G interactions per SoC, whereas Anton

---

[*] https://www.psc.edu/resources/computing/anton

is reported to run MD simulations on proteins that are up to 2 orders of magnitude faster than that achieved using state-of-the-art CPUs.

One advantage of using the SoC is that more specialised network topologies can be adopted. For example, in Anton there are 6x network links, allowing each processor to exchange data about changes to the neighbouring subdomains with a neighbouring processor using a dedicated bidirectional link of over 100Gbps bandwidth. Thus, the hardware network topology can very closely match that of the spatial decomposition used to parallelise the MD code. This is very difficult to achieve using commodity hardware.

2.5. High-performance computing and gains expected in simulation runtime

The use of high-performance computation or simply HPC has transcended the use of MD and many other simulation techniques. This has allowed scaling of the simulation length scales to meet the experimental lower limits and has brought the run time of simulation much faster than individual workstations. For example, currently, significant work is being undertaken at the Lawrence Livermore National laboratory in conducting large scale atomic simulations with the integrated usage of the "Dislocation extraction algorithm" (DXA) and Crystal analysis tool (CAT) [23] for studying metal plasticity, crystal defects, dislocation lines and their Burgers Vectors from the MDS output data [24]. In Europe, the most common way of requesting the use of a HPC for MD is via the PRACE project call [25]. PRACE is an international non-profit entity that bridges 26 member states to rapidly accelerate scientific discoveries by offering access to world-leading supercomputers from various European countries such as ARCHER (UK), Hazel Hen, SuperMuc and Juwels (Germany), Joliot (France), Marconi (Italy), MareNostrum (Spain) and Piz Daint (Switzerland). To efficiently use high-performance computing, it is very important to benchmark the results at an early stage to identify the most optimal number of processing threads or nodes for specific simulations. It is often the case that the performance obtained in a simulation on an HPC can only scale up efficiently up to a certain

number of CPU cores beyond which the communication overhead associated with message passing between cores becomes more time consuming than the numerical processing on each core. As an example, some data on certain machines and certain force fields (potential functions) benchmarked by LAMMPS developers [26]. As another example on scaling of a large range bond order potential function on the UK's supercomputer ARCHER reveals that the optimal scaling of LAMMPS MD can be made up to about 100 nodes or 2400 cores (currently, ARCHER has 24 cores/node) where the performance scales linearly before degrading as shown in figure 4. However, when the same performance was tested on the Isambard HPC, it was found that the performance of long-range screened bond order potentials [27] (referred as the atomistica library) [28] scaled all the way upto 10,000 cores as opposed to the Tersoff potential where the performance degraded beyond 2000 Cores. This performance gain is an architecture-dependent feature, which is why every HPC needs to be benchmarked separately. What's noticeable here is that the linear slope of ideal gain presented by the ARCHER HPC and Isambard HPC are different, which explains the power gain (strength) of each HPC.
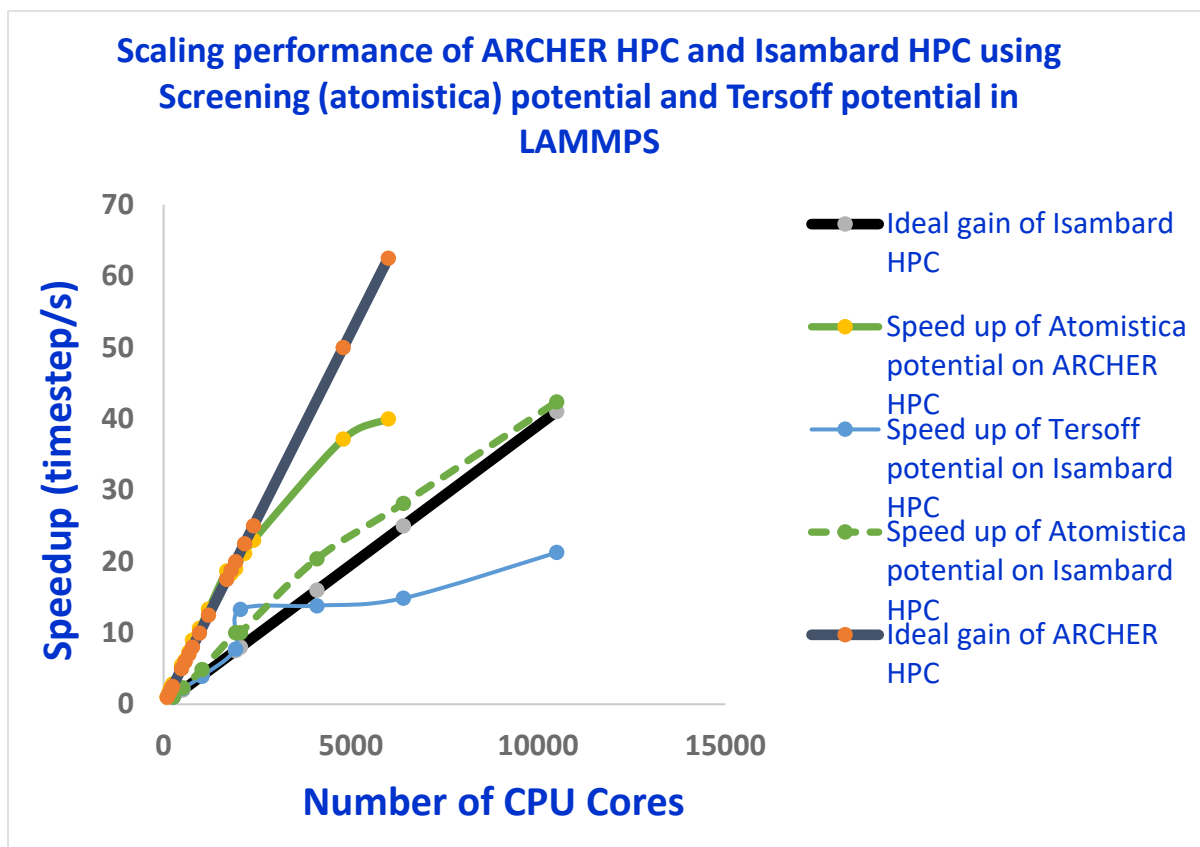
Figure 4: Scaling performance of bond order potentials on two HPC's (Note that ARCHER HPC (http://www.archer.ac.uk/) contains 24 cores/node whilst Isambard HPC contains 64 cores/node (https://gw4.ac.uk/isambard/)

Typically, for micromachining and other contact loading simulations, the velocity of the tool or the probe is an important consideration in deciding the time length of the simulation run. For instance, if one would use a velocity of 20 m/sec to achieve a length of cut of 2 nm with free travel of the tool of 0.5 nm while approaching the workpiece then it takes about 125 ps of simulation time as shown in table 1. Note that for a pair potential like the Morse potential this job can take as little as 3 to 4 hours but for a more complicated potential (such as Screening REBO), a similar calculation can take two orders of magnitude longer to calculate.

Table 1: Sample calculation for estimating the number of timesteps required for an MD run

Speed of cutting	20 m/s = 0.02 nm/ps
Total simulation time	(2+0.5 nm)/0.02 nm/ps = 125 ps
Timestep for each calculation	2 fs = 0.002 ps
Total run timesteps	125 ps/0.002 ps = 62,500 cycles

3.0 Case studies of simulation applications in advanced nano-manufacturing areas

3.1. Introduction to Solid freeform fabrication (SFF)

The need to have denser, lightweight and faster electronic gadgets has resulted in the development of compact semiconductor products with advanced functions that incorporate devices into a thin package. These needs are met by system-in-package (SiP) products, which are competing in parallel with Package-on-Package (PoP) products, where multiple chips are stacked in a single package. The scaling down of these products to sub 10 nm wiring intervals poses extreme challenges in assessing manufacturing quality and device performance. This increasingly stringent manufacturing scenario requires tight control in the testing of semiconductor devices. Agile and low-cost methods for characterisation of electrical performance are sought by a multitude of electronic industries. The unprecedented accuracies sought in terms of depth control is to allow layer by layer removal of material (with ~1 nm depth control) and to perform simultaneous electrical device characterisation. Consequently, a vast range of microfabrication techniques, either standalone [29], sequential [30] or hybrid methods [31] are fast developing. Modern assembly line product manufacturing in the precision sector cannot rely on either subtractive (such as micromachining) or additive (laser processing) manufacturing alone. Thus, a new area in fabrication making combined use of additive manufacturing and/or subtractive manufacturing techniques is emerging which is referred to as "Solid freeform fabrication". The simplest example of SFF is that of a microdrill used for precision hole making operations. A drill has a complex flute shape which is first finished by

micromachining (subtractive manufacturing) to achieve the right shape and then coated (additive manufacturing) to achieve longevity in its cutting performance. Consequently, as the products in modern engineering applications are reaching the utmost complexities in terms of precision, the manufacturing issues faced therein are realised to be far more complex than what is seen in micromanufacturing processes. A vast number of other similar examples exist, biomedical prosthetic implants (of CoCr, stainless steel or Ti6Al4V), for instance, are usually ground and polished and subsequently coated with materials like hydroxyapatite (HA) or a telescopic mirror is usually ground and polished to achieve tight form before being subjected to an additive optical coating.

A more recent precision solid freeform fabrication technology called Roll-to-Roll fabrication (R2R) [32] as shown in Figure 5 (one of the large R2R platform developed at Cranfield University) is being increasingly used these days.

Precision machined copper drum

Micro-gratings fabricated on drum for embossing the polymer film

Injection slot die for coating the polymer sheet that is cured by UV light after embossing

Polymer film (~100 μm thick PET) to be embossed

Granite bed
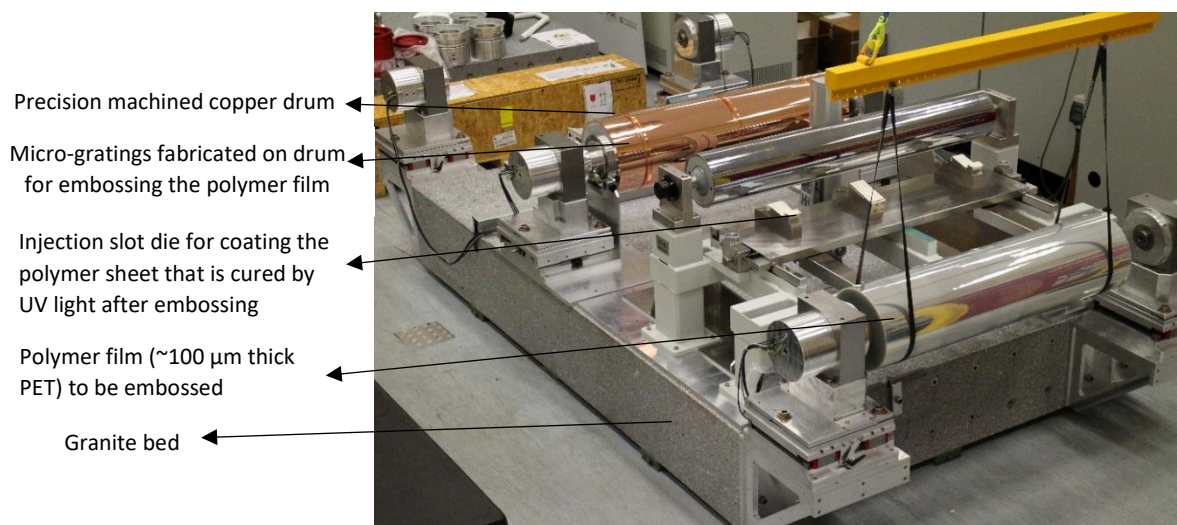
Figure 5: A manufacturing platform R2R built at Cranfield University to accommodate 1.6 m width production capacity

Products that are produced with R2R include 1) Next generation displays (flexible or large-scale), activated and animated wall coverings, 3D displays, intelligent packaging and innovative clothing; 2) Pharmaceutical technologies; 3) Plastic electronics supporting a range

of low cost consumer products from food packaging to hand held devices; 4) Photovoltaics, energy and energy harvesting devices. Interruptions caused during large scale production of these high-value products may succumb to time/energy/materials losses if the process is not well-controlled. The intent of using R2R is to rapidly fabricate polymer films for a wide range of applications including, for example, television displays as shown in Figure 6.

a) Optical design   (b) subtractive machining of drum   (c) R2R additive fabrication using drum
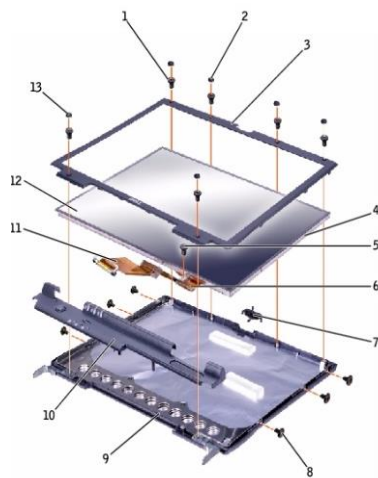
(d) assembly of fabricated products   (e) consumer application

Figure 6: An assembly of design to manufacturing precision processes (a-e) via R2R

One can see that complex engineering products usually rely on an intelligent combination of a range of techniques comprising both subtractive and additive technologies. The scope of this review vastly covers technologies about advances in subtractive and additive technologies such as electrochemical micromachining, electrochemical spark micromachining, electrochemical microtexturing, diamond turn micromachining and various deposition-based manufacturing

processes.

The photovoltaic industry leads renewable energy generation with annual production in year 2018 reaching ~100 GW out of overall renewable power of 181 GW. Currently, c-Si is the undisputed market leader with a share of over 90% capable of achieving grid parity in major sectors. The conventional additive/ subtractive manufacturing processes are the hallmark of c-Si technology, but the major limitation is the energy intensive processing requiring large investment of few billions such as silicon extraction from raw materials and high-volume manufacturing to stay in competition for the affordable cost of electricity. However, the total share of all modern renewables is only 2% including solar, wind, biomass, geothermal and ocean power. Clearly, there is a need of efficient, durable, disruptive and affordable PV technologies involving non-toxic and abundant materials which can be easily processed at low capital investment. Mature inorganic thin film technologies viz. Cadmium Telluride (CdTe), and copper indium diselenide ($CuInGaSe_2$) or CIGS solar cells are two major commercial successes. CIGS solar cells can be processed on rigid (glass) and flexible substrate (metal or polymer foils) with great potential to compete with c-Si technology, using R2R processing with proper thermal management as shown in figure 7.
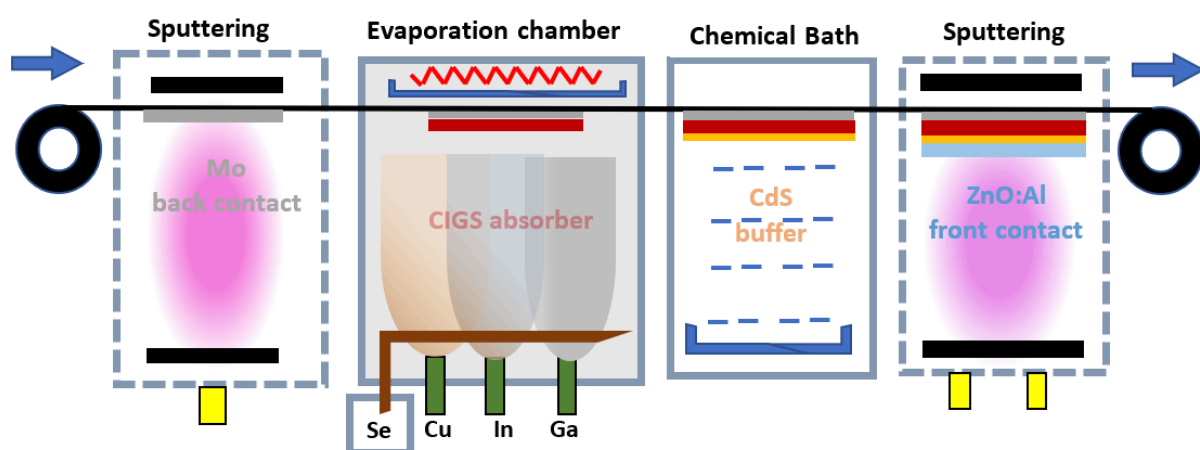
Figure 7: A schematic for R2R deposition of CIGS solar cell on metal or polymer foil through various stages of back contact: Molybdenum deposition by sputtering, absorber CIGS using effusion cells of Cu, In and Ga metals in selenium environment, CdS buffer layer using PVD/ Chemical Bath Deposition and front contact transparent conducting oxide ZnO: Al

The process shown in figure 7 when implemented on R2R suffers from manufacturing challenges of processing at 450 °C to 550 °C on a roll, thus the turn-key process solution does not exist at large scale volume production on flexible foils.

Figure 8 shows a photograph of an in-line pilot system designed and developed for high performance CIGS solar cells over the 30 cm × 30 cm area on glass substrates jointly developed by London South Bank University and Scientific Vacuum Systems Ltd. (SVS).


Figure 8: A photograph showing an in-line pilot system for high performance CIGS solar cells through sequential layer deposition using a robotic arm without breaking vacuum.

The processed solar cells of large areas over 30 cm × 30 cm can be converted into a module using a combined additive process of deposition of layers and subtractive processes of using laser scribing process in sequential steps to form a mini-module with a number of series connected cells as shown below in figure 9.
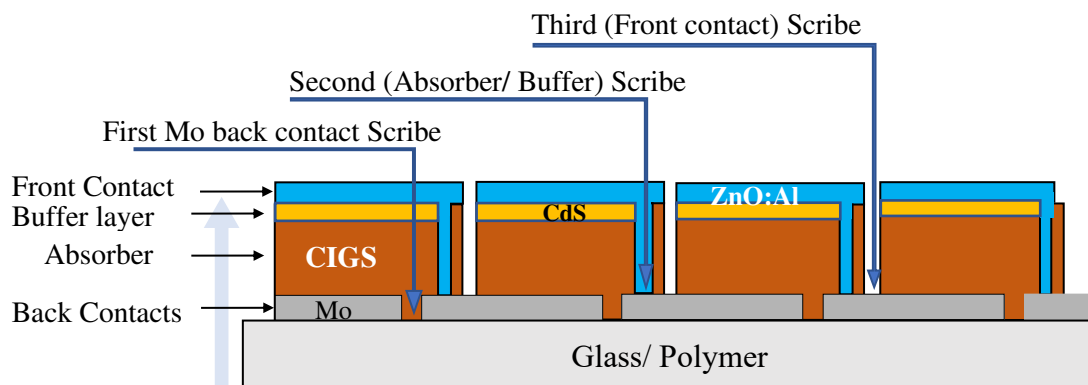
(a)
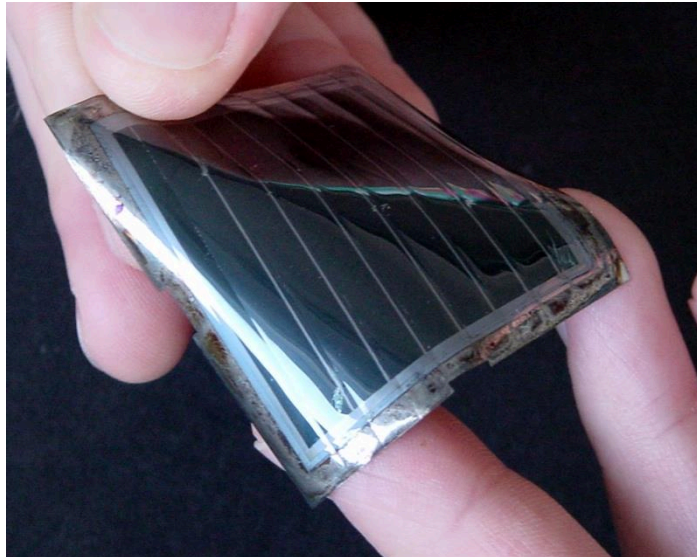
(b)

Figure 9: (a) A schematic of a monolithic module design for CIGS solar cells in series connections using sequential laser scribing steps as shown above and (b) photograph of a CIGS minimodule representing a series connection of eight CIGS solar cell strips. Reprinted with permission [33]

Besides these, new generation disruptive Organic Solar Cells are the candidates, which are showing some great promise recently, particularly the hybrid (organic/ inorganic) Perovskite solar cells have achieved unprecedented energy conversion efficiencies from ~4% to ~25%, within a decade but suffer from stability issues to guarantee the life time of the module for > 20 years. Efforts are underway to further enhance the performance using tandem solar cell combination in an attempt to achieve conversion efficiencies over 30%. Nevertheless, Organic Solar Cells have recently made an excellent jump in conversion efficiency numbers reaching around the 18% mark, which makes it a near commercial possibility with low upfront cost (CAPEX). However, the issues of long-term stability still remain a challenge as the active layers undergo degradation under atmospheric oxygen and moisture, which will require engineering challenges to be overcome such as price and durability of sealing materials or strategies for required successful commercialisation of the technology.

Figure 10 below represents a multijunction (or tandem) organic solar cell with a multiple stack

of three absorber materials with blue absorber on top, green in the middle and red as the bottom cell, all connected in series in a 2-terminal monolithic configuration.
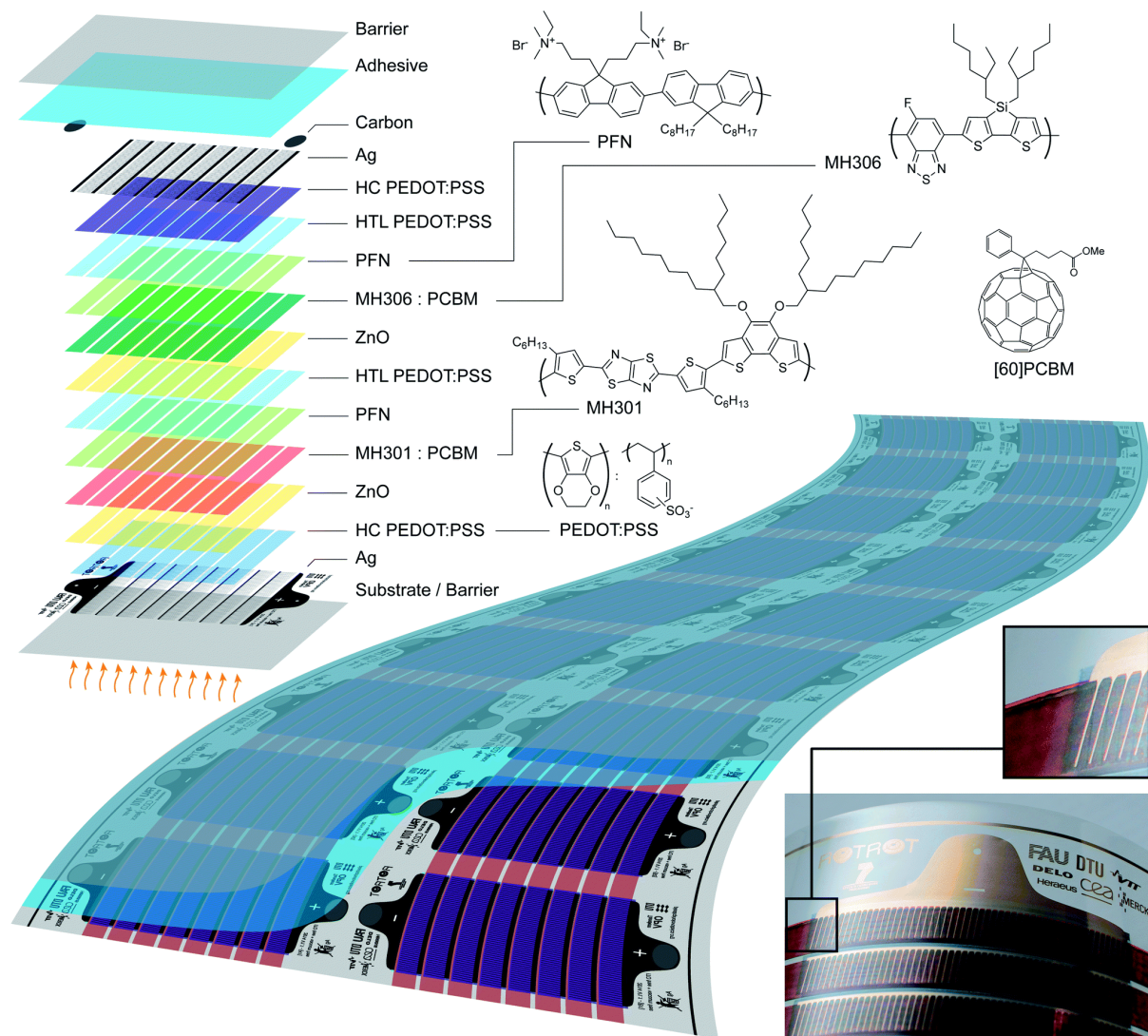

Figure 10: A 14-layer tandem stack (upper left) along with structural formulae and names for the different materials involved (top right). The outline of the printed web is shown (middle) along with an actual photograph of a module (lower right). In the close-up photograph, the differently coloured active materials (red colour from MH301, green colour from MH306 and blue colour from PEDOT: PSS) are seen representing the wide band gap and low band gap semiconductor junctions and the hole transport layer. Reprinted with permission [34]

3.1.1. Simulation application in advance subtractive manufacturing processes

The need to adopt simulations in the study of subtractive (as well as additive) micromanufacturing processes stems from the complex interfacial interaction between the tool and the workpiece. A schematic representation of this complex interaction behaviour - taking

place at an interface or in its immediate vicinity comprising of mechanical (solid and fluid), thermal, electro-magnetic, metallurgical, quantum and other effects is shown in figure 11.
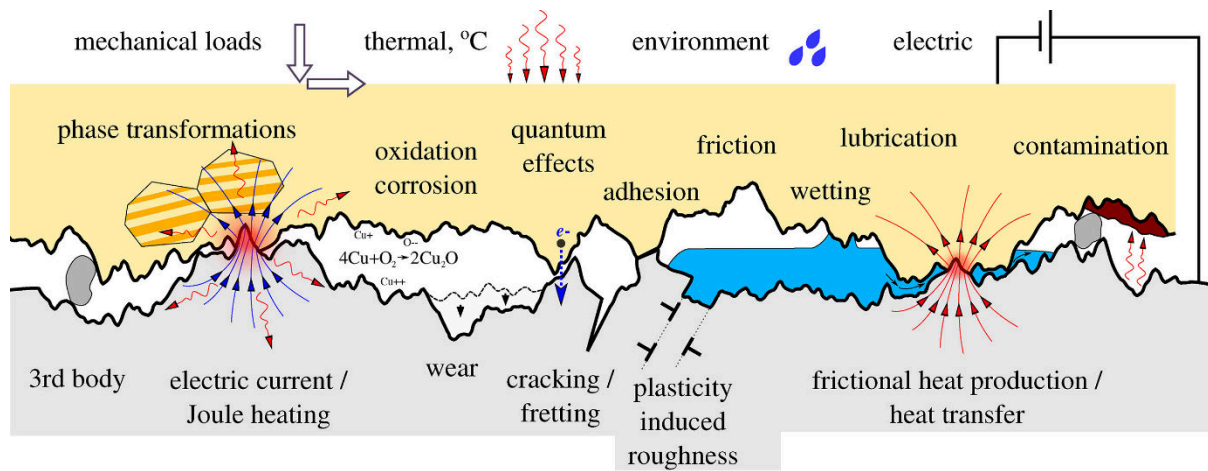

Figure 11: Schematic representation of the non-linear multi-functional nature of physical, chemical and mechanical interactions at the interface of two moving asperities commonly seen during a contact loading condition in presence of environmental effects, Reprinted with permission [9]

Traditionally, MD simulation of micromachining or other contact loading processes (such as nanoindentation) assumes an indenter to be a smooth, rigid and otherwise inert body impenetrable by other bodies, particularly because the focus of the investigation remains on the deformation of the substrate (workpiece) rather than the cutting tool. This assumption is widespread in the atomistic simulation studies of nanoindentation [35, 36] as well as nanometric cutting or nanoscratching [37, 38]. This assumption of having a rigid indenter in MD has been implemented by following one of the three cases: (a) assuming a rigid diamond indenter (carbon atoms), (b) assuming a rigid indenter comprising of the atoms of the same material of the substrate and (c) assuming an imaginary spherical rigid repulsive indenter described by a force of magnitude $F(r) = -K(r-R)^2$ ($r < R$) where K is the force constant and R is the radius of the indenter. An attempt was recently made for the first time to compare these situations and it was found, interestingly, that even when an indenter is considered rigid, the near-surface phenomena such as cohesion or adhesion are always active, and this can trigger

changes in the way incipient plasticity is induced in the substrate [10]. The aforementioned study is a prime example highlighting the importance of material interaction and description of the tool atoms as much as that of the substrate even when a tool is considered rigid during the simulation. A lot of review articles are now available focussing on studying material-specific theories including metals [39, 40], ceramics like silicon carbide [38] as well as semiconductors like silicon [41, 42]. More recently advanced applications of MD have been made to explore elliptical vibration-assisted machining [43], laser ablation [44] and wire electrical discharge machining (EDM) [45].

Besides these, other historic reviews provide nice details on the art of micromachining both using experiments and MD simulations [46-48]. A more appropriate effort would be to perform MD simulation of the cutting process in the presence of water molecules (see Figure 12). The interatomic potential function now exists for doing such studies [49, 50].
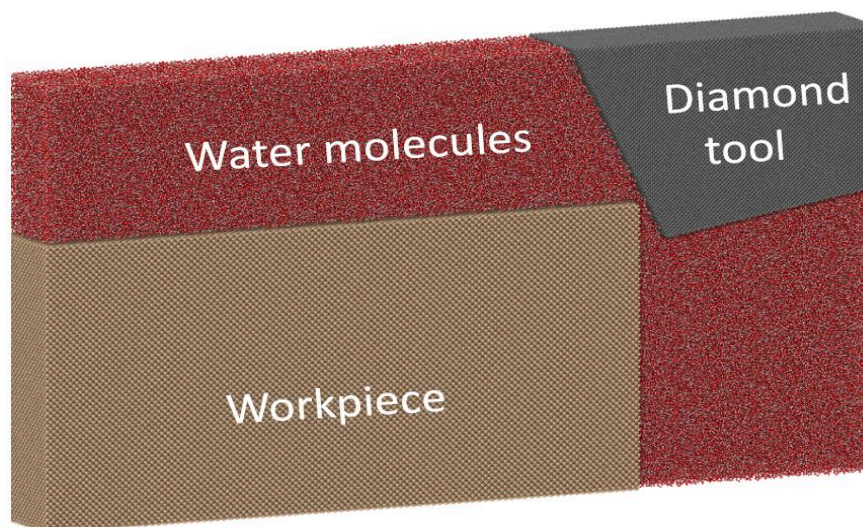

Figure 12: MD simulation of the cutting process of silicon in the presence of H_2O molecules

3.1.2. MD simulation application in additive or deposition-based manufacturing processes

There are various material deposition processes whereby our fundamental understanding of material interactions is lacking, and the use of simulations is increasingly growing. These include both vacuum-based and non-vacuum-based deposition processes for example,

sputtering, etching and implantation. Figure 13(a) shows an example of the simulated deposition process showing how clusters of atoms align themselves during a growth process. Simulations of melt or vapor-phase growth also provide a strong means of assessing the transferability and robustness of a potential function as it presents a variety of local configurations and complex combinations of the stoichiometry of compounds under various temperature and pressure conditions [51]. More recently, MD simulation has also been used to understand the influence of initial velocity and particle temperature during thermal spraying in the resulting splat formation (see figure 13b).

Ti, Ag and O atoms being deposited on a Ti slab
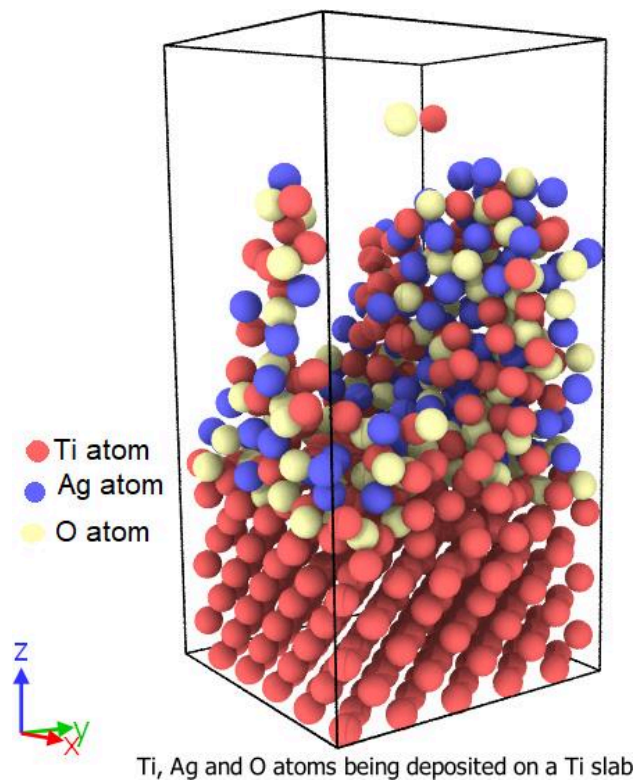
(a)
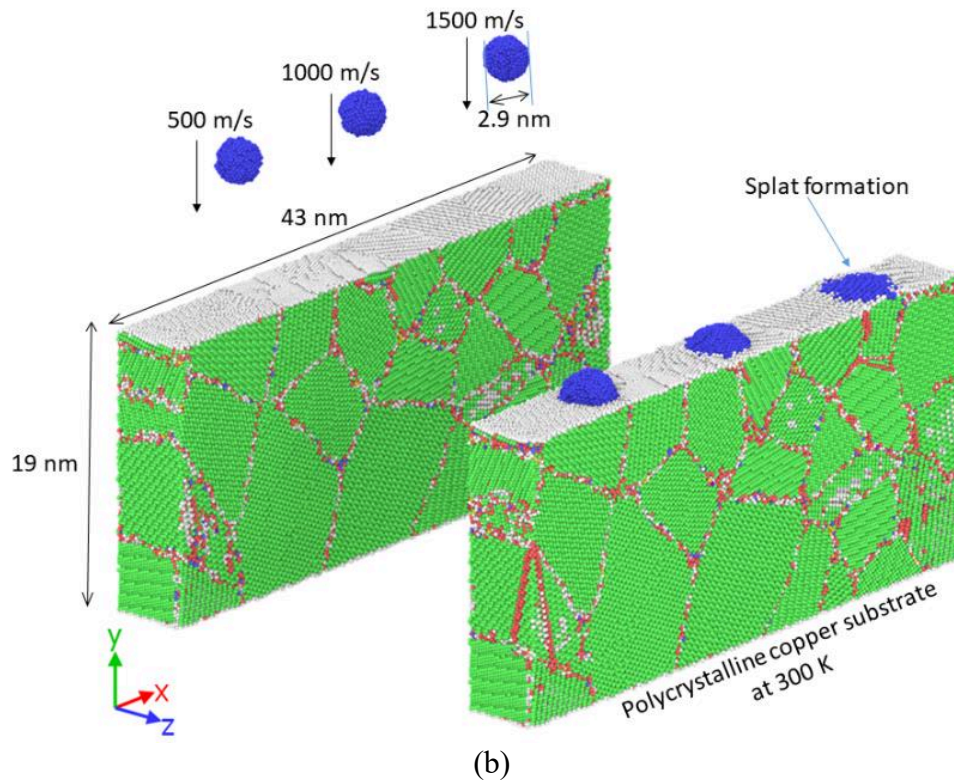
Figure 13: (a) MD simulation of deposition (growth) of titanium, silver and oxygen atoms on a titanium substrate (unpublished work by the authors), (b) splat formation during thermal spray deposition of copper on a polycrystalline copper substrate at various velocities. Reprinted with permission [52]

The numerical deposition of Giant magnetoresistive (GMR) multilayers is a successful example. GMR multilayers are composed of two magnetic layers sandwiching a conductive copper layer. GMR read head sensors for hard disk drives have been the enabling technologies for laptops since late last century, but their initial development encountered a challenge: the conductive layer must be thin (~20 Å) and yet must have uniform thickness with sharp interfaces. Interestingly, high energy processes (e.g., sputtering) created better GMR devices than the more refined molecular beam epitaxy (MBE) processes. MD simulations indicated that high energy impacts can flatten the surface [53], but this also creates mixed interface especially when the second magnetic layer is grown on the soft copper layer, figure 14(b). This prediction was validated by the 3D atom probe (3DAP) experiment shown in figure 14(a) [54]. MD was then used to demonstrate that when a low energy is used to deposit the first few atomic planes of a new layer to avoid mixing, a subsequent high energy can be used to grow the

23

remaining layer to flatten the surface [54] as shown in figure 14(c). This results in the development of biased target ion beam deposition (BTIBD) technology that uses modulated energy to improve GMR multilayers [55].
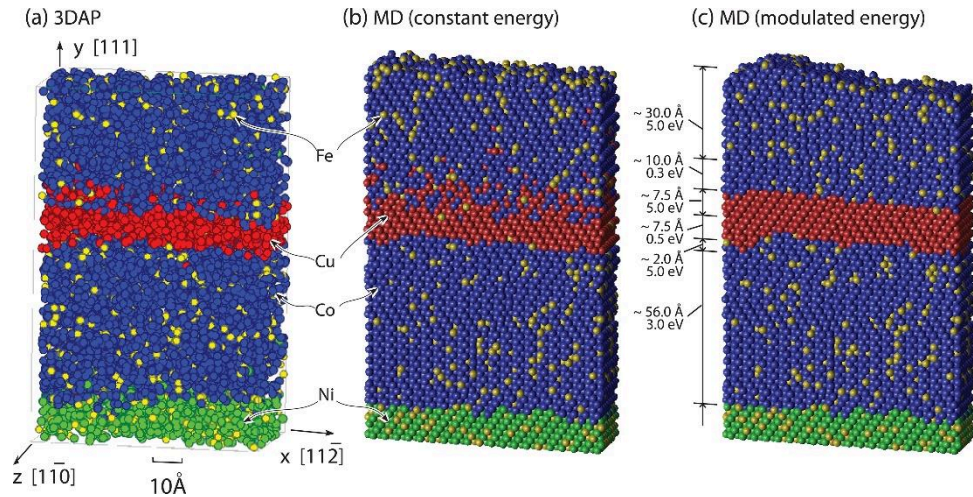

Figure 14: Atomic configuration of GMR multilayers obtained from (a) 3D atom probe (2DAP) experiment, (b) constant energy MD simulation, and (c) modulated energy MD simulation. Reprinted with permission [54]

On the same note, atomic scale growth of more complex semiconductor compound multilayers HgTe/CdSe/ZnS has been simulated using MD [56] (see figure 15a) and the deposition of plutonium on carbon was studied under varying conditions (figure 15b) [57]. These simulations revealed detailed formation mechanisms of various defects including misfit dislocations and stacking faults without any prior assumptions about these defects. They provide an effective means to guide experiments to reduce these defects.

(a)
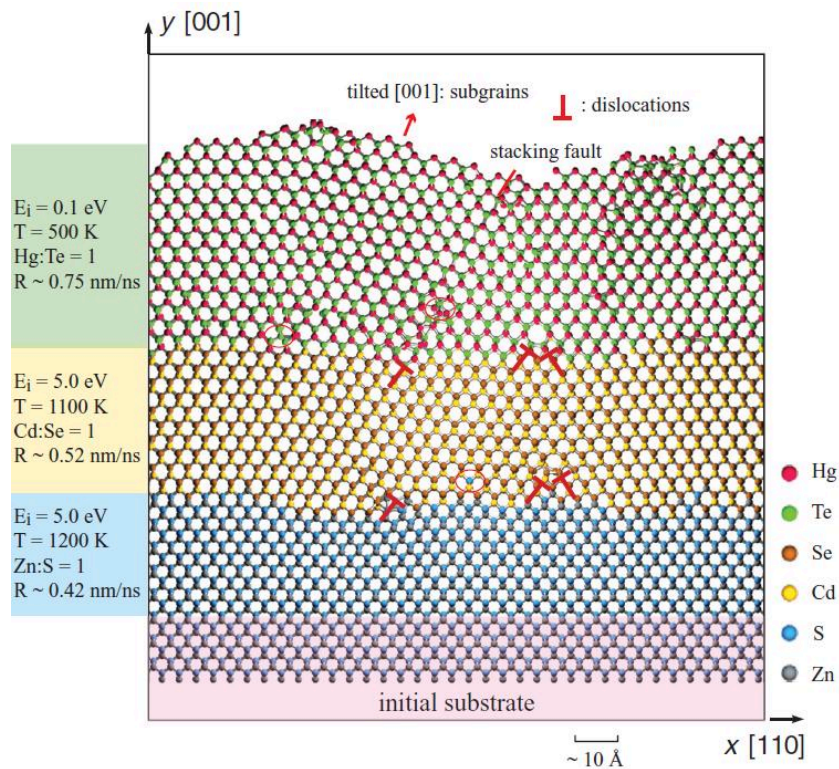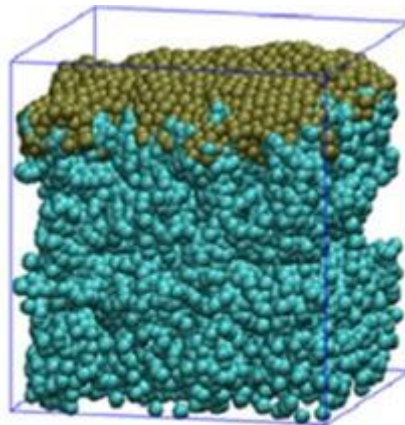
$E_{deposit} = 0.02 GeV$

(b)

Figure 15: (a) atomic scale growth of the HgTe/CdSe/ZnS multilayers obtained from molecular dynamics simulation where the pink shaded area highlights the initial ZnS substrate [56], and (b) deposition of plutonium on porous carbon substrate. Reprinted with permission [57]

As one good example, figures 16(a) and 16(b) show MD simulations of GaN growth in [0001] and [11$\bar{2}$0] directions respectively [58, 59] where the initial substrate, wurtzite, zinc-blende, and defective (i.e., undefinable) regions are shown in black, orange, blue, and white colours respectively. Almost defect-free structures can be grown in the [11$\bar{2}$0] growth direction (except

for the surface which is coloured white), but significant defects (including alteration of wurtzite and zinc-blende regions) exist in the [0001] growth direction. This is because the (11$\bar{2}$0) stacking is ABAB … which means that on a given plane of A, adatoms can only fall on B sites. Contrarily, the (0001) stacking is ABCABC … so that on a given plane A, adatoms can either occupy the correct sites B or the defective sites C, resulting in significant defects. This understanding can be used to control crystal structures through careful seeding. For instance, the (110) stacking of a zinc-blende structure is ABAB … so one can use a (110) zinc-blende seeding to force the film to grow into a zinc-blende structure.
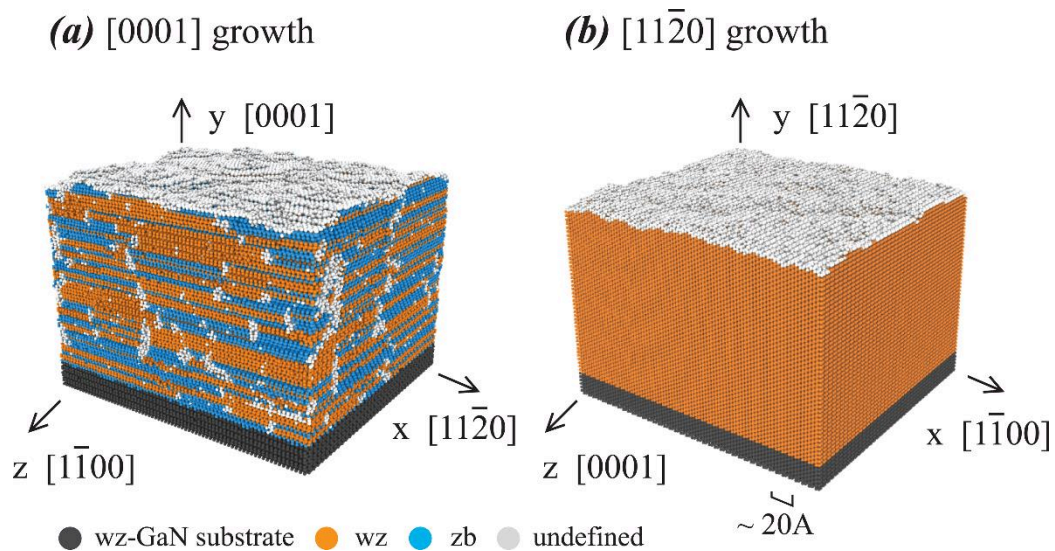

Figure 16: MD simulated atomic configurations of GaN files grown in (a) [0001] and (b) [11$\bar{2}$0] directions Reprinted with permission [58, 59].

Overall as additive manufacturing or coatings are predicted to be shaping the future of micromanufacturing to enable wealth of human life, the use of simulations to make these processes more deterministic is going to continue to play a crucial role.

4.0. Ongoing developments in MD simulation

4.1.1. Building complex crystal structures

The starting point in doing MD simulation is to build a crystal lattice structure. For simple, building BCC, FCC, HCP and diamond cubic lattices is straightforward, but in practice, we

often face materials with rather complex crystal structures. Thanks to the Materials Genome Initiative, a database now exists which is significantly helpful in predicting certain crystal structures [60]. Besides this source, Big data analytic tools are also helping towards this drive and significant information is now available to help early-stage MD researchers in building the crystal lattice structure more easily [61-63]. An additional database exists [64] to predict phase properties of materials which clarifies phase change mechanisms such as those occurring during cutting of brittle materials.

4.1.2. Development of potential energy functions or force field

A potential function is the backbone of an MD simulation and the evolution of these over the years is reviewed in detail in various sources [29, 65, 66]. MRS Bulletin (Volume 37, Issue 5, 2012) released a special issue titled "Three decades of many-body potentials in materials research"[†]. Various pioneers in the area of MD contributed to this issue to elucidate a long lineage on the development of potential functions (force fields) including Tersoff, embedded atomic method (EAM), bond order potential (BOP), reactive empirical bond order (REBO) and so on. It has already been highlighted that a potential function is usually just suitable for a specific material or to a specific process whether the material is based on carbon [67, 68], silicon [69, 70] or tungsten [71]. It is pertinent to note that a good evaluation and assessment of the potential function is required and ideally a potential should be carefully selected for simulations involving large strain deformations such as those seen during contact loading operations like nanoindentation or nanoscratching [10]. A more recently growing trend in the area of development of potential functions is the use of the machine learning approach [72], although several codes exist, such as atomicrex [73] that allow parametrising the potential function based on the wisdom of the researcher.

[†] https://www.cambridge.org/core/journals/mrs-bulletin/issue/three-decades-of-manybody-potentials-in-materials-research

Conclusions

This review sheds light on the immense and imminent opportunities available for scholars to leverage high-performance computing simulation tools for the benefit of applied knowledge in various areas of engineering. The recently published papers reviewed here have shed light on the need for a deeper understanding of the linkages between materials science and applied commercial manufacturing. Areas related to solid freeform fabrication encompassing examples from additive manufacturing such as coating deposition, thermal spray as well as subtractive manufacturing including diamond machining and nanotribology have been largely benefited by the advance knowledge in the simulation field. This knowledge is becoming richer with the growing use of national computing resources and is enabling researchers to attain unprecedented unapproachable limits in manufacturing. Scalability in simulations is as big of a challenge as scalability in the manufacturing of precision components *e.g.*, patterned surfaces in metals. However, some of these challenges can now be tackled with newly emerging dedicated computational hardware solutions and this is immensely benefitting the field of materials science-oriented precision manufacturing.

References:

[1] J. Longbottom, J. Lanham, Cutting temperature measurement while machining–a review, Aircraft Engineering and Aerospace Technology 77(2) (2005) 122-130.

[2] S. Pervaiz, I. Deiab, E.M. Wahba, A. Rashid, M. Nicolescu, A coupled FE and CFD approach to predict the cutting tool temperature profile in machining, Procedia CIRP 17 (2014) 750-754.

[3] R. Gracie, T. Belytschko, An adaptive concurrent multiscale method for the dynamic simulation of dislocations, Int J Numer Meth Eng 86(4-5) (2011) 575-597.

[4] C. Oskay, J. Fish, Fatigue life prediction using 2-scale temporal asymptotic homogenization, Int J Numer Meth Eng 61(3) (2004) 329-359.

[5] P. Kerfriden, J.C. Passieux, S.P.A. Bordas, Local/global model order reduction strategy for the simulation of quasi-brittle fracture, Int J Numer Meth Eng 89(2) (2012) 154-179.

[6] S.G. Psakhie, Y. Horie, S.Y. Korostelev, A.Y. Smolin, A.I. Dmitriev, E.V. Shilko, S.V. Alekseev, Method of movable cellular automata as a tool for simulation within the framework of mesomechanics, Russ Phys J 38(11) (1995) 1157-1168.

[7] Y. Tan, D. Yang, Y. Sheng, Discrete element method (DEM) modeling of fracture and damage in the machining process of polycrystalline SiC, J Eur Ceram Soc 29(6) (2009) 1029-1037.

[8] H.M. Pen, Y.C. Liang, X.C. Luo, Q.S. Bai, S. Goel, J.M. Ritchie, Multiscale simulation of nanometric cutting of single crystal copper and its experimental validation, Comp Mater Sci 50(12) (2011) 3431-3441.

[9] A.I. Vakis, V.A. Yastrebov, J. Scheibert, L. Nicola, D. Dini, C. Minfray, A. Almqvist, M. Paggi, S. Lee, G. Limbert, J.F. Molinari, G. Anciaux, R. Aghababaei, S. Echeverri Restrepo, A. Papangelo, A. Cammarata, P. Nicolini, C. Putignano, G. Carbone, S. Stupkiewicz, J. Lengiewicz, G. Costagliola, F. Bosia, R. Guarino, N.M. Pugno, M.H. Müser, M. Ciavarella, Modeling and simulation in tribology across scales: An overview, Tribol Int 125 (2018) 169-199.

[10] S. Goel, G. Cross, A. Stukowski, E. Gamsjäger, B. Beake, A. Agrawal, Designing nanoindentation simulation studies by appropriate indenter choices: Case study on single crystal tungsten, Comp Mater Sci 152 (2018) 196-210.

[11] D. Shaw, M. Deneroff, R. Dror, J. Kuskin, R. Larson, J. Salmon, C. Young, B. Batson, K. Bowers, J. Chao, Proceedings of the ACM/IEEE Conference on Supercomputing (SC09), ACM Press New York, 2009.

[12] M. Allen, D. Tildesley, Computer Simulation of Liquids Oxford University Press Oxford 385, (1987).

[13] T. Darden, D. York, L. Pedersen, Particle mesh Ewald: An N· log (N) method for Ewald sums in large systems, The Journal of chemical physics 98(12) (1993) 10089-10092.

[14] R.W. Hockney, J.W. Eastwood, Computer simulation using particles, crc Press1988.

[15] E. Pollock, J. Glosli, Comments on P3M, FMM, and the Ewald method for large periodic Coulombic systems, Comput Phys Commun 95(2-3) (1996) 93-110.

[16] J.C. Phillips, R. Braun, W. Wang, J. Gumbart, E. Tajkhorshid, E. Villa, C. Chipot, R.D. Skeel, L. Kale, K. Schulten, Scalable molecular dynamics with NAMD, J Comput Chem 26(16) (2005) 1781-1802.

[17] S. Plimpton, Fast Parallel Algorithms for Short-Range Molecular Dynamics, J Comput Phys 117 (1995) 1-19.

[18] D.A. Case, T. Darden, T. Cheatham III, C. Simmerling, J. Wang, R. Duke, R. Luo, R. Walker, W. Zhang, K. Merz, AMBER 12; University of California: San Francisco, 2012, There is no corresponding record for this reference 1-826.

[19] B.R. Brooks, A program for macromolecular energy, minimization, and dynamics calculations, J Comput Chem 4 (1983) 187-217.

[20] R. Fine, G. Dimmler, C. Levinthal, FASTRUN: a special purpose, hardwired computer for molecular simulation, Proteins: Structure, Function, and Bioinformatics 11(4) (1991) 242-253.

[21] T. Narumi, Y. Ohno, N. Okimoto, T. Koishi, A. Suenaga, N. Futatsugi, R. Yanai, R. Himeno, S. Fujikawa, M. Taiji, A 55 TFLOPS simulation of amyloid-forming peptides from yeast prion Sup35 with the special-purpose computer system MDGRAPE-3, Proceedings of the 2006 ACM/IEEE conference on Supercomputing, ACM, 2006, p. 49.

[22] I. Ohmura, G. Morimoto, Y. Ohno, A. Hasegawa, M. Taiji, MDGRAPE-4: a special-purpose computer system for molecular dynamics simulations, Phil. Trans. R. Soc. A 372(2021) (2014) 20130387.

[23] S. Goel, B. Beake, C.-W. Chan, N. Haque Faisal, N. Dunne, Twinning anisotropy of tantalum during nanoindentation, Materials Science and Engineering: A 627(0) (2015) 249-261.

[24] L.A. Zepeda-Ruiz, A. Stukowski, T. Oppelstrup, V.V. Bulatov, Probing the limits of metal plasticity with molecular dynamics simulations, Nature 550(7677) (2017) 492.

[25] https://prace-ri.eu/ accessed on 27/2/2020.

[26] https://lammps.sandia.gov/bench.html accessed on 27/7/2020.

[27] L. Pastewka, A. Klemenz, P. Gumbsch, M. Moseler, Screened empirical bond-order potentials for Si-C, Phys Rev B 87(20) (2013) 205410.

[28] https://github.com/Atomistica/atomistica accessed on 27/7/2020.

[29] S. Goel, X. Luo, A. Agrawal, R.L. Reuben, Diamond machining of silicon: A review of advances in molecular dynamics simulation, International Journal of Machine Tools and Manufacture 88(0) (2015) 131-164.

[30] S.Z. Chavoshi, S. Goel, P. Morantz, Current trends and future of sequential micro-machining processes on a single machine tool, Mater Design 127 (2017) 37-53.

[31] S.Z. Chavoshi, X. Luo, Hybrid micro-machining processes: A review, Precision Engineering 41(Supplement C) (2015) 1-23.

[32] Roll to Roll (R2R) Processing Technology Assessment available from https://www.energy.gov/sites/prod/files/2015/02/f19/QTR%20Ch8%20-%20Roll%20To%20Roll%20Processing%20TA%20Feb-13-2015.pdf accessed on 27/7/2020.

[33] H. Upadhayaya, T. Razykov, A. Tiwari, Photovoltaics fundamentals, technology and application, Handbook of Energy Efficiency Renewable Energy (2007) 23.

[34] T.R. Andersen, H.F. Dam, M. Hösel, M. Helgesen, J.E. Carlé, T.T. Larsen-Olsen, S.A. Gevorgyan, J.W. Andreasen, J. Adams, N. Li, Scalable, ambient atmosphere roll-to-roll manufacture of encapsulated large area, flexible organic tandem solar cell modules, Energy & Environmental Science 7(9) (2014) 2925-2933.

[35] Y. Mo, K.T. Turner, I. Szlufarska, Friction laws at the nanoscale, Nature 457(7233) (2009) 1116-1119.

[36] J. Belak, Nanotribology: Modelling Atoms When Surfaces Collide, Energy and Technology Review, Lawrence Livermore Laboratory, 1994.

[37] T. Zykova-Timan, D. Ceresoli, E. Tosatti, Peak effect versus skating in high-temperature nanofriction, Nat Mater 6(3) (2007) 230-234.

[38] S. Goel, A topical review on "The current understanding on the diamond machining of silicon carbide", Journal of Physics D: Applied Physics 47(24) (2014) 243001.

[39] I.A. Alhafez, C.J. Ruestes, Y. Gao, H.M. Urbassek, Nanoindentation of hcp metals: a comparative simulation study of the evolution of dislocation networks, Nanotechnology 27(4) (2015) 045706.

[40] C.J. Ruestes, I.A. Alhafez, H.M. Urbassek, Atomistic Studies of Nanoindentation—A Review of Recent Advances, Crystals 7(10) (2017) 293.

[41] L.N. Abdulkadir, K. Abou-El-Hossein, A.I. Jumare, M.M. Liman, T.A. Olaniyan, P.B. Odedeyi, Review of molecular dynamics/experimental study of diamond-silicon behavior in nanoscale machining, The International Journal of Advanced Manufacturing Technology 98(1) (2018) 317-371.

[42] L.N. Abdulkadir, K. Abou-El-Hossein, A.I. Jumare, P.B. Odedeyi, M.M. Liman, T.A. Olaniyan, Ultra-precision diamond turning of optical silicon—a review, The International Journal of Advanced Manufacturing Technology (2018) 1-36.

[43] S. Goel, F.D. Martinez, S.Z. Chavoshi, N. Khatri, C. Giusca, Molecular dynamics simulation of the elliptical vibration-assisted machining of pure iron, Journal of Micromanufacturing 1(1) (2018) 6-19.

[44] A.P. Markopoulos, D.E. Manolakos, Ablation study of laser micromachining process with molecular dynamics simulation, Proceedings of the Institution of Mechanical Engineers, Part B: Journal of Engineering Manufacture 231(3) (2017) 415-426.

[45] T. Roy, A. Sharma, D. Datta, R. Balasubramaniam, Molecular dynamics study on the effect of discharge on adjacent craters on micro EDMed surface, Precision Engineering 52 (2018) 469-476.

[46] R. Komanduri, L. Raff, A review on the molecular dynamics simulation of machining at the atomic scale, Proceedings of the Institution of Mechanical Engineers, Part B: Journal of Engineering Manufacture 215(12) (2001) 1639-1672.

[47] X. Liu, R.E. DeVor, S.G. Kapoor, K.F. Ehmann, The Mechanics of Machining at the

Microscale: Assessment of the Current State of the Science, Journal of Manufacturing Science and Engineering 126(4) (2004) 666-678.

[48] P.J. Arrazola, T. Özel, D. Umbrello, M. Davies, I.S. Jawahir, Recent advances in modelling of metal machining processes, CIRP Annals - Manufacturing Technology 62(2) (2013) 695-718.

[49] J.D. Schall, J.A. Harrison, Reactive Bond-Order Potential for Si-, C-, and H-Containing Materials, The Journal of Physical Chemistry C 117(3) (2013) 1323-1334.

[50] J. Seppä, B. Reischl, H. Sairanen, V. Korpelainen, H. Husu, M. Heinonen, P. Raiteri, A.L. Rohl, K. Nordlund, A. Lassila, Atomic force microscope adhesion measurements and atomistic molecular dynamics simulations at different humidities, Measurement Science and Technology 28(3) (2017) 034004.

[51] D. Ward, X. Zhou, B. Wong, F. Doty, J. Zimmerman, Accuracy of existing atomic potentials for the CdTe semiconductor compound, The Journal of chemical physics 134(24) (2011) 244703.

[52] S. Goel, N.H. Faisal, V. Ratia, A. Agrawal, A. Stukowski, Atomistic investigation on the structure–property relationship during thermal spray nanoparticle impact, Comp Mater Sci 84(0) (2014) 163-174.

[53] X. Zhou, H. Wadley, Atomistic simulations of the vapor deposition of Ni/Cu/Ni multilayers: The effects of adatom incident energy, J Appl Phys 84(4) (1998) 2301-2315.

[54] X. Zhou, H. Wadley, R.A. Johnson, D. Larson, N. Tabat, A. Cerezo, A. Petford-Long, G. Smith, P. Clifton, R. Martens, Atomic scale structure of sputtered metal multilayers, Acta Mater 49(19) (2001) 4005-4015.

[55] T. Hylton, B. Ciorneiu, D. Baldwin, O. Escorcia, J. Son, M. McClure, G. Waters, Thin film processing by biased target ion beam deposition, Ieee T Magn 36(5) (2000) 2966-2971.

[56] X. Zhou, D. Ward, J. Martin, F. van Swol, J. Cruz-Campa, D. Zubia, Stillinger-Weber potential for the II-VI elements Zn-Cd-Hg-S-Se-Te, Phys Rev B 88(8) (2013) 085309.

[57] E.C. Neyts, P. Brault, Molecular Dynamics Simulations for Plasma-Surface Interactions, Plasma Processes and Polymers 14(1-2) (2017) 1600145.

[58] J. Gruber, X. Zhou, R. Jones, S. Lee, G. Tucker, Molecular dynamics studies of defect formation during heteroepitaxial growth of InGaN alloys on (0001) GaN surfaces, J Appl Phys 121(19) (2017) 195301.

[59] K. Chu, J. Gruber, X. Zhou, R. Jones, S. Lee, G. Tucker, Molecular dynamics studies of InGaN growth on nonpolar (11$\bar{2}$0) GaN surfaces, Physical Review Materials 2(1) (2018) 013402.

[60] https://www.materialsproject.org/ accessed on 27/7/2020.

[61] https://analytics-toolkit.nomad-coe.eu/home/ accessed on 27/7/2020.

[62] http://www.geocities.jp/ohba_lab_ob_page/structure1.html accessed on 27/7/2020.

[63] http://rruff.geo.arizona.edu/AMS/amcsd.php accessed on 27/7/2020.

[64] http://resource.npl.co.uk/mtdata/mtdatasoftware.htm accessed on 27/7/2020.

[65] J.A. Harrison, J.D. Schall, S. Maskey, P.T. Mikulski, M.T. Knippenberg, B.H. Morrow, Review of force fields and intermolecular potentials used in atomistic computational materials research, Applied Physics Reviews 5(3) (2018) 031104.

[66] J.A. Harrison, M. Fallet, K.E. Ryan, B.L. Mooney, M.T. Knippenberg, J.D. Schall, Recent developments and simulations utilizing bond-order potentials, Model Simul Mater Sc 23(7) (2015) 074003.

[67] C. de Tomas, I. Suarez-Martinez, N.A. Marks, Graphitization of amorphous carbons: A comparative study of interatomic potentials, Carbon 109 (2016) 681-693.

[68] S. Goel, A. Stukowski, Comment on "Incipient plasticity of diamond during nanoindentation" by C. Xu, C. Liu and H. Wang, RSC Advances, 2017, 7, 36093, RSC Advances 8(10) (2018) 5136-5137.

[69] S.Z. Chavoshi, S. Xu, S. Goel, Addressing the discrepancy of finding the equilibrium melting point of silicon using molecular dynamics simulations, Proceedings of the Royal Society A: Mathematical, Physical and Engineering Science 473(2202) (2017).

[70] Z. Zhang, A. Stukowski, H.M. Urbassek, Interplay of dislocation-based plasticity and phase transformation during Si nanoindentation, Comp Mater Sci 119 (2016) 82-89.

[71] D. Cereceda, A. Stukowski, M. Gilbert, S. Queyreau, L. Ventelon, M. Marinica, J. Perlado, J. Marian, Assessment of interatomic potentials for atomistic analysis of static and dynamic properties of screw dislocations in W, Journal of Physics: Condensed Matter 25(8) (2013) 085702.

[72] L. Hu, R. Su, B. Huang, F. Liu, An Accurate and Transferable Machine-Learning Interatomic Potential for Silicon, arXiv preprint arXiv:1901.01638 (2019).

[73] A. Stukowski, E. Fransson, M. Mock, P. Erhart, Atomicrex—a general purpose tool for the construction of atomic interaction models, Model Simul Mater Sc 25(5) (2017) 055003.